



Ultrasound delivery of a TrkA agonist confers neuroprotection to Alzheimer-associated pathologies

✉ Kristiana Khima,^{1,2} Kelly Markham-Coultes,¹ ✉ Rikke Hahn Kofoed,¹
✉ H. Uri Saragovi,^{3,4,5} Kullervo Hynynen^{6,7} and ✉ Isabelle Aubert^{1,2}

Early degeneration of basal forebrain cholinergic neurons contributes substantially to cognitive decline in Alzheimer's disease. Evidence from preclinical models of neuronal injury and aging support a pivotal role for nerve growth factor (NGF) in neuroprotection, resilience, and cognitive function. However, whether NGF can provide therapeutic benefit in the presence of Alzheimer's disease-related pathologies still unresolved. Perturbations in the NGF signalling system in Alzheimer's disease may render neurons unable to benefit from NGF administration. Additionally, challenges related to brain delivery remain for clinical translation of NGF-based therapies in Alzheimer's disease. To be safe and efficient, NGF-related agents should stimulate the NGF receptor, tropomyosin receptor kinase A (TrkA), avoid activation through the p75 neurotrophin receptor (p75^{NTR}), and be delivered non-invasively to targeted brain areas using real-time monitoring. We addressed these limitations using MRI-guided focused ultrasound (MRIgFUS) to increase blood–brain barrier permeability locally and transiently, allowing an intravenously administered TrkA agonist that does not activate p75^{NTR}, termed D3, to enter targeted brain areas. Here, we report the therapeutic potential of selective TrkA activation in a transgenic mouse model that recapitulates numerous Alzheimer's disease-associated pathologies. Repeated MRIgFUS-mediated delivery of D3 (D3/FUS) improved cognitive function in the TgCRND8 model of Alzheimer's disease. Mechanistically, D3/FUS treatment effectively attenuated cholinergic degeneration and promoted functional recovery. D3/FUS treatment also resulted in widespread reduction of brain amyloid pathology and dystrophic neurites surrounding amyloid plaques. Furthermore, D3/FUS markedly enhanced hippocampal neurogenesis in TgCRND8 mice, implicating TrkA agonism as a novel therapeutic target to promote neurogenesis in the context of Alzheimer's disease-related pathology. Thus, this study provides evidence that selective TrkA agonism confers neuroprotection to effectively counteract Alzheimer's disease-related vulnerability. Recent clinical trials demonstrate that non-invasive blood–brain barrier modulation using MRIgFUS is safe, feasible and reversible in Alzheimer's disease patients. TrkA receptor agonists coupled with MRIgFUS delivery constitute a promising disease-modifying strategy to foster brain health and counteract cognitive decline in Alzheimer's disease.

- 1 Hurvitz Brain Sciences Research Program, Biological Sciences, Sunnybrook Research Institute, Toronto, ON M4N 3M5, Canada
- 2 Department of Laboratory Medicine and Pathobiology, University of Toronto, Toronto, ON M5S 1A8, Canada
- 3 Lady Davis Institute, Jewish General Hospital, Montreal, QC H3T 1E2, Canada
- 4 Department of Pharmacology and Therapeutics, McGill University, Montreal, QC H3G 1Y6, Canada
- 5 Department of Ophthalmology and Vision Sciences, McGill University, Montreal, QC H4A 3S5, Canada
- 6 Physical Sciences, Sunnybrook Research Institute, Toronto, ON M4N 3M5, Canada
- 7 Department of Medical Biophysics, University of Toronto, Toronto, ON M5G 1L7, Canada

Received April 08, 2021. Revised October 01, 2021. Accepted November 19, 2021. Advance access publication December 17, 2021

© The Author(s) 2022. Published by Oxford University Press on behalf of the Guarantors of Brain.

This is an Open Access article distributed under the terms of the Creative Commons Attribution-NonCommercial License (<https://creativecommons.org/licenses/by-nc/4.0/>), which permits non-commercial re-use, distribution, and reproduction in any medium, provided the original work is properly cited. For commercial re-use, please contact journals.permissions@oup.com

Correspondence to: Isabelle Aubert
Sunnybrook Research Institute
2075 Bayview Avenue, Rm. S112
Toronto, ON, M4N 3M5, Canada
E-mail: isabelle.aubert@sri.utoronto.ca; isabelle.aubert@utoronto.ca

Keywords: tropomyosin receptor kinase A; focused ultrasound; drug delivery; basal forebrain cholinergic neurons; Alzheimer's disease

Abbreviations: ACh = acetylcholine; AChE = acetylcholinesterase; BBB = blood–brain barrier; BFCN = basal forebrain cholinergic neuron; ChAT = choline acetyltransferase; MRIgFUS = MRI-guided focused ultrasound; MS/DBB = medial septum/diagonal band of Broca; NBM = nucleus basalis; NGF = nerve growth factor; p75^{NTR} = p75 neurotrophin receptor; TrkA = tropomyosin receptor kinase A

Introduction

The vulnerability of basal forebrain cholinergic neurons (BFCNs) contributes to cognitive dysfunction in individuals with Alzheimer's disease.¹ Acetylcholinesterase (AChE) inhibitors, which prevent acetylcholine (ACh) breakdown in the synaptic cleft, are currently approved as symptomatic therapies for Alzheimer's disease and their long-term use may also have disease-modifying benefits.^{2–4} Eventually, however, the underlying cholinergic neurodegeneration becomes severe, and efforts to bolster ACh levels at the synaptic cleft can no longer mask denervation. In this regard, nerve growth factor (NGF), essential for BFCN survival, function and plasticity, is being pursued as a therapeutic agent for Alzheimer's disease. NGF has the potential to prevent cholinergic degeneration, stimulate ACh synthesis and release from remaining neurons, and thus could have a significant impact on the clinical progression of Alzheimer's disease.¹

Effective clinical translation of NGF-based therapeutic strategies remains a challenge. To date, NGF-based therapeutics have failed to impact cognition in Alzheimer's disease clinical trials. However, some patients showed increased cholinergic sprouting and upregulation of phenotypic cholinergic markers, implicating a therapeutic benefit of NGF in patients with Alzheimer's disease.^{5–10} Clinical efficacy may be limited due to impaired NGF signalling mechanisms in Alzheimer's disease patients and/or technical constraints related to therapeutic delivery.^{10–16} Specifically, NGF binds to two receptors, tropomyosin receptor kinase A (TrkA) and p75 neurotrophin receptor (p75^{NTR}), known—in some circumstances—to mediate opposing biological effects: cell survival and cell death, respectively.¹¹ Pro-survival TrkA is downregulated in Alzheimer's disease, which may favour NGF binding to p75^{NTR} and ultimately contribute to cholinergic dysfunction.¹⁷ Additionally, in the presence of Alzheimer's disease pathology, deficits in NGF metabolism compromise the conversion of proNGF to mature NGF, leading to increased extracellular levels of proNGF.¹¹ ProNGF preferentially interacts with p75^{NTR} to mediate neuronal degeneration.¹¹ Taken together, these pathways may negate the benefit of TrkA activation by NGF in the Alzheimer's disease brain. Thus, therapeutics designed to maximize TrkA activation, without engaging p75^{NTR}, may achieve optimal neuroprotection of BFCNs in Alzheimer's disease.

One such pharmacological agent, D3, is a peptidomimetic agonist of TrkA that promotes neuronal survival, neurite extension and cholinergic tone.^{18–21} However, like NGF, compound D3 does not cross the blood–brain barrier (BBB), which represents a major obstacle for non-invasive delivery to the brain. To date, NGF-related clinical trials have relied on invasive intracranial procedures that carry substantial risk of surgery-related complications, including intracranial haemorrhage and tissue injury.^{9,13} In addition,

accurate dosing, spatial targeting and distribution could not be confirmed or controlled following surgical delivery of a gene vector producing NGF or a device encapsulating NGF-secreting cells.^{6,9,15} Recent post-mortem histological analysis revealed the challenges and importance of accurate stereotactic targeting and the limitation of NGF distribution in Alzheimer's disease brains.¹⁴ Real-time imaging and monitoring of drug delivery to the brain will be critical for effective clinical application.

To circumvent these translational limitations, we recently established the feasibility of administering intravenous D3 with MRI-guided focused ultrasound (MRIgFUS), to transiently increase BBB permeability in the basal forebrain, thereby delivering D3 to targeted brain areas.^{21,22} This approach led to enhanced cholinergic activity in the TgCRND8 mouse model of amyloidosis.²¹ In this study, we aimed to determine whether non-invasive, selective TrkA stimulation is sufficient to impact cognitive decline in the presence of Alzheimer's disease-related pathology, namely amyloid- β accumulation, cholinergic dysfunction and neurotrophic deficits. We developed a treatment paradigm using MRIgFUS-mediated delivery of D3 that stimulated functional cholinergic innervation to target regions, increased hippocampal neurogenesis, reduced amyloid- β pathology, ultimately converging on improved cognition in a mouse model of amyloidosis that mimics the cholinergic deficits seen in Alzheimer's disease.

Materials and methods

Animals

Sex-balanced, age-matched TgCRND8 mice and non-Tg mice were used in this study. TgCRND8 mice express hAPP695 with the Swedish (KM670/671NL) and Indiana (V717F) mutations under the control of the hamster prion gene promoter. Mice were bred on a hybrid C57BL/6-C3H background.²³ TgCRND8 mice were randomized to experimental groups as follows: (i) D3/FUS-treated (16 mg/kg intravenous D3 and MRIgFUS); (ii) PBS/FUS-treated (intravenous PBS and MRIgFUS); (iii) D3-treated (16 mg/kg intravenous D3, no MRIgFUS); or (iv) PBS-treated (intravenous PBS, no MRIgFUS). Phosphate-buffered saline (PBS)-treated, non-Tg mice were used to control for genotype. Mice were maintained under a 12-h light/dark cycle with free access to food and water. All animal procedures were approved by the Sunnybrook Research Institute Animal Care Committee and conducted in accordance with Canadian Council on Animal Care guidelines. All behavioural, biochemical and histopathological assessments were conducted by investigators blinded to experimental group.

TrkA ligand

The selective TrkA ligand D3 (MedChemExpress, HY-17622) was analysed for purity with HPLC (> 98% pure) prior to use in this study. A detailed pharmacological characterization is provided in Maliartchouk et al.¹⁸

MRI-guided focused ultrasound

MRIgFUS was performed as previously described, using an in-house prototype system (commercialized as LP100, FUS Instruments Inc.).²¹ Spatial coordinates of the transducer positioning system were co-registered to a 7.0 T MRI (Bruker), allowing FUS targeting from structural MRI. T₂-weighted images were used to bilaterally target the basal forebrain in a first sonication, then the hippocampus and cortex in a second sonication. An inter-sonication interval of 5 min allowed microbubbles to be cleared from the circulation. During the first sonication, mice received a tail vein injection of D3 (16 mg/kg) diluted in PBS or PBS only and Definity microbubbles (0.02 ml/kg; Lantheus Medical Imaging). In the second sonication, animals received another dose of Definity and Gadovist (0.2 ml/kg, Bayer). Each injectable was followed by a 150 µl saline flush for transfer into the bloodstream.

Acoustic emissions were recorded using an in-house manufactured PZT hydrophone and coupled to a feedback controller. The applied pressure was increased step-wise after each pulse until the magnitude of subharmonic acoustic emissions passed 3.5 times the mean of baseline. The applied pressure was reduced to 50% and maintained at this level for the rest of the sonication. Peak pressure was calculated for each target and averaged across all targets within an animal.

BBB permeability was confirmed by an increase in Gadovist signal intensity on T₁-weighted images obtained 5 min after the second sonication. Percent enhancement was quantified as the mean pixel intensity in a 2 mm × 2 mm voxel region of interest corresponding to each target spot relative to an untreated reference region and averaged across all focal spots within an animal (MATLAB).

Behavioural testing

All behavioural testing was performed during the light phase of the cycle by an experimenter blinded to the treatment. Behavioural procedures are detailed in the [Supplementary material](#).

Biochemical assays for cholinergic function

Mice were anaesthetized, decapitated, and the brains were rapidly dissected on ice. Dissected medial septum/diagonal band of Broca (MS/DBB) and nucleus basalis (NBM) were flash-frozen and stored at –80°C. Choline acetyltransferase (ChAT) activity was measured by incorporation of ¹⁴C-acetyl-CoA into ¹⁴C-ACh, as previously described.²¹ Dissected hippocampus and cortex were frozen at –80°C until assayed for AChE activity using the Amplex Red detection kit (Invitrogen). Freshly dissected hippocampus and cortex were separated into 500 µm transverse slices for evaluation of basal and potassium-evoked ACh release.²¹ Tissue ACh and choline were extracted from freshly dissected hippocampus and cortex as described.²⁴ The final ACh and choline content were determined using the Amplex Red detection kit (Invitrogen). Radioactivity was measured using liquid scintillation counting (Beckman Coulter). Protein content was determined using the bicinchoninic acid assay (Thermo Scientific).

Immunohistochemistry and imaging

Mice were deeply anaesthetized with ketamine/xylazine (CDMV). Animals were intracardially perfused with saline followed by 4% paraformaldehyde. Brains were removed, post-fixed in 4% paraformaldehyde for 24 h at 4°C, then placed in 30% sucrose. Coronal, 40 µm brain sections were prepared using a sliding microtome (Leica) and stored at –20°C in cryoprotectant buffer. Free-floating sections were rinsed with 0.1 M PBS, then incubated in blocking solution (PBS with 0.3% Triton X-100 and 10% donkey serum) for 1 h at room temperature. Sections were incubated for 72 h at 4°C with the following primary antibodies: goat anti-ChAT (1:500; EMD Millipore, AB144P), mouse anti-BrdU (1:400; ExBio, 11-286-C100), rabbit anti-DCX (1:200; Abcam, ab207175), guinea pig anti-NeuN (1:500; EMD Millipore, ABN90), mouse 6F3D anti-amyloid-β (1:200; Dako, M0872). Brain sections were rinsed with PBS, then incubated with fluorescently conjugated secondary antibodies (1:200; Jackson ImmunoResearch) and DAPI (1:15000; Invitrogen) for 2 h at room temperature. Amyloid plaques were labelled with 1% Thioflavin S for 7 min, followed by two sequential incubations in 70% ethanol for 5 min. For bromodeoxyuridine (BrdU) staining, antigen retrieval was performed by incubating sections in 2 N HCl for 30 min at 37°C. Acid was neutralized in borate buffer (pH 8.5) for 10 min. For doublecortin (DCX) staining, Tris-EDTA buffer (pH 8.0) at 80°C for 40 min was used for antigen retrieval.

Immunofluorescence was visualized with a Nikon A1 laser scanning confocal microscope and images were acquired with NIS-Elements software (Nikon). Z-stack images were acquired with 2, 1 and 0.2 µm optical thickness using the 10×, 20× and 60× objectives, respectively. Quantitative image analyses were performed while blinded to treatment groups.

Statistical analysis

Prism 8 software (GraphPad) was used for statistical analysis. All values are expressed as the means ± standard error of the mean (SEM). Two groups were compared using unpaired Student's t-tests. For analysis of unshredded nest material between groups, we used the Kruskal-Wallis test with the Dunn *post hoc* method. The following outcome measures were analysed using repeated measures two-way ANOVA: nesting score, Barnes Maze learning and search strategy score, contrast enhancement, peak pressure during sonication and body weight. ChAT+ fibre density, DCX+ Sholl crossings and plaque distribution analysis were assessed by two-way ANOVA. All other parameters were analysed using a one-way ANOVA. The Holm-Sidak *post hoc* test was used for multiple comparisons in statistically significant ANOVAs. Correlation was performed using linear regression analysis with 95% confidence intervals. *P* < 0.05 was set as threshold for statistical significance.

Data availability

Additional data related to this paper are available from the corresponding author upon reasonable request.

Results

MRIgFUS-mediated delivery of D3 improves cognition in TgCRND8 mice

The TgCRND8 model is an aggressive, early-onset model of amyloidosis. Significant amyloid-β plaque pathology and cognitive deficits emerge by 3 months.²³ Regional progression of plaque

pathology is similar to that seen in Alzheimer's disease, beginning in the cortex and spreading to the hippocampus, olfactory bulbs, and thalamus by 4 months.^{23,25} Aberrant amyloid- β accumulation induces cortical and hippocampal synaptic loss, neuronal network dysfunction and degeneration.^{23,26–30} Functional cholinergic deficits are also apparent in TgCRND8 mice by 4 months.^{21,31–34} Bellucci *et al.* reported cholinergic cell loss in the basal forebrain by 7 months, with significant shrinkage of remaining cholinergic cell bodies and neurites.³¹ Consistent with these findings, we demonstrate the presence of earlier BFCN atrophy, decreased cholinergic innervation, and cholinergic dystrophic neurites by 5 months of age (Supplementary Fig. 1). Five-month-old TgCRND8 mice also exhibit deficits in hippocampal neurogenesis, including decreased proliferation, differentiation and survival of newborn neurons.^{35,36} Here, D3/FUS treatment was initiated in 5-month-old TgCRND8 mice, when cognitive impairment and Alzheimer's disease-associated pathologies, including amyloid deposition, cholinergic degeneration and neurogenesis deficits, are already well established.

We first examined whether selective TrkA stimulation with D3, combined with MRIgFUS delivery, could promote cognitive function. Mice at 5 months of age were treated once per week for three consecutive weeks, followed by behavioural testing (Fig. 1A–D). We examined nest building to evaluate daily living activity, a novel object recognition task to assess recognition memory, Y maze to measure spatial working memory and Barnes maze for spatial reference memory and cognitive flexibility.

By 6.5 months of age, TgCRND8 mice present with substantial amyloid burden and cognitive deficits.²³ TgCRND8 mice showed poor nest construction compared to non-Tg littermates (Fig. 1E). Nest building was improved by D3/FUS treatment relative to PBS/FUS and D3-treated controls (Fig. 1E and Supplementary Fig. 2A). D3/FUS-treated TgCRND8 mice also shredded more nesting material than PBS/FUS and D3-treated TgCRND8 mice, comparable to non-Tg mice (Supplementary Fig. 2B). The nest building behaviour of TgCRND8 mice prior to the first treatment was balanced after treatment groups were randomized (Supplementary Fig. 2C and D).

In the novel object recognition test, D3-treated TgCRND8 demonstrated impaired recognition memory, without preferential exploration of a novel object over a familiar one (Fig. 1F and Supplementary Fig. 3A). D3/FUS-treated mice performed better than D3 and PBS/FUS-treated mice in demonstrating their preference for the novel object, comparable to non-Tg controls (Fig. 1F and Supplementary Fig. 3B). Novelty-seeking behaviour as measured by total object exploration time was unaffected by treatment (Fig. 1G and Supplementary Fig. 3C). No differences in locomotor behaviour were observed across groups (Supplementary Fig. 3D and E).

In the Y maze, spontaneous alternation was used as an index of spatial working memory. The performance of D3/FUS-treated mice was comparable to non-Tg littermates and significantly better than D3 and PBS/FUS-treated TgCRND8 mice (Fig. 1H). Exploratory activity assessed by search density (Supplementary Fig. 4A) and total entries into the arms did not differ between groups (Fig. 1I). No differences in average velocity and distance travelled were observed across treatments (Supplementary Fig. 4B and C). Prior to the first treatment, TgCRND8 mice allocated to different experimental conditions demonstrated similar performance in Y maze alternation (Supplementary Fig. 4D–G).

Mice from all groups were able to learn the location of an escape box in the Barnes maze over a 4-day training period (Fig. 2A). However, the performance of D3-treated TgCRND8 mice was worse compared to non-Tg mice in the acquisition phase, indicating a

genotype deficit in learning this task (Fig. 2A). Distance travelled followed a similar trend as latency to escape (Supplementary Fig. 5A). Motor performance was unaffected across trials (Supplementary Fig. 5B). Spatial search strategies were classified (Fig. 2B) and assigned a relative score based on spatial learning (Fig. 2C). Non-Tg mice shifted from random and serial navigation on Day 1 towards more efficient, spatial navigation on Day 4 (Fig. 2C and D). In contrast, D3-treated TgCRND8 mice relied mostly on random and serial navigation over all trial days (Fig. 2C and D). On Day 5, the escape box was removed to test memory recall (Fig. 2E–H). D3-treated TgCRND8 mice spent less time in the target zone than non-Tg mice (Fig. 2F) and exhibited a higher number of errors (i.e. the number of entries to a non-target hole) (Fig. 2G and Supplementary Fig. 5C and D). Analysis of navigation strategy in the probe trial indicated that D3-treated TgCRND8 mice used less spatially-dependent strategies than non-Tg mice (Fig. 2H). D3/FUS-treated mice showed comparable learning to non-Tg mice (Fig. 2A–D) and bias for the target zone in the probe trial (Fig. 2E–H). No effect of FUS alone was observed (Fig. 2A–H).

Mice were subsequently trained in a reversal learning paradigm. D3-treated TgCRND8 mice demonstrated impaired reversal learning (Fig. 2I) and lower mean spatial navigation scores compared to non-Tg mice (Fig. 2J). Unlike non-Tg mice, D3-treated TgCRND8 mice adopted predominantly random and serial search strategies (Fig. 2K). Distance travelled followed a similar trend as latency to escape (Supplementary Fig. 6A). No differences were observed in mean speed during reversal learning across treatment groups, ruling out *a priori* differences in locomotor activity (Supplementary Fig. 6B). During the reversal probe trial, TgCRND8 mice spent less time in the target zone than non-Tg mice (Fig. 2L and Supplementary Fig. 6C) and relied on non-spatial navigation (Fig. 2M). There was an increase in number of errors made by D3-treated TgCRND8 mice relative to non-Tg controls (Supplementary Fig. 6D–F). D3/FUS-treated mice showed improvement in reversal learning performance indicating that cognitive flexibility is restored (Fig. 2I–M). Altogether, these findings indicate that repeated D3/FUS, relative to D3 and PBS/FUS treatments, led to improved performance in cognitive tasks. It is important to note that D3/FUS enhanced cognitive function in the context of mid-stage amyloid pathology and Alzheimer's disease-related neurotrophic deficits, further supporting the translational potential of this work.

D3/FUS rescues BFCNs and associated pathways in TgCRND8 mice

Next, we sought to evaluate the potential neural mechanisms underlying improved cognitive function following D3/FUS treatment. To examine the structure and function of BFCNs, the MS/DBB and NBM subregions of the basal forebrain were immunostained for ChAT, the enzyme responsible for ACh synthesis (Fig. 3A). In both the MS/DBB and NBM, no difference in the numbers of ChAT+ cells were detected across experimental conditions (Fig. 3B). However, D3/FUS-treated TgCRND8 mice exhibited an increase in the ChAT+ soma size (Fig. 3C), extension (Fig. 3D), surface area (Fig. 3E) and branching (Fig. 3F) of ChAT+ neurites, relative to PBS, D3 and FUS-treated mice. D3/FUS also increased ChAT enzyme activity in the MS/DBB and NBM of TgCRND8 mice, relative to D3 and PBS/FUS alone (Fig. 3G).

To determine whether changes in the BFCN soma were accompanied by changes in their terminal fields, we examined ChAT+ fibres in the hippocampus and cortex (Fig. 4). Non-Tg mice exhibited an extensive network of cholinergic fibres in the hippocampus

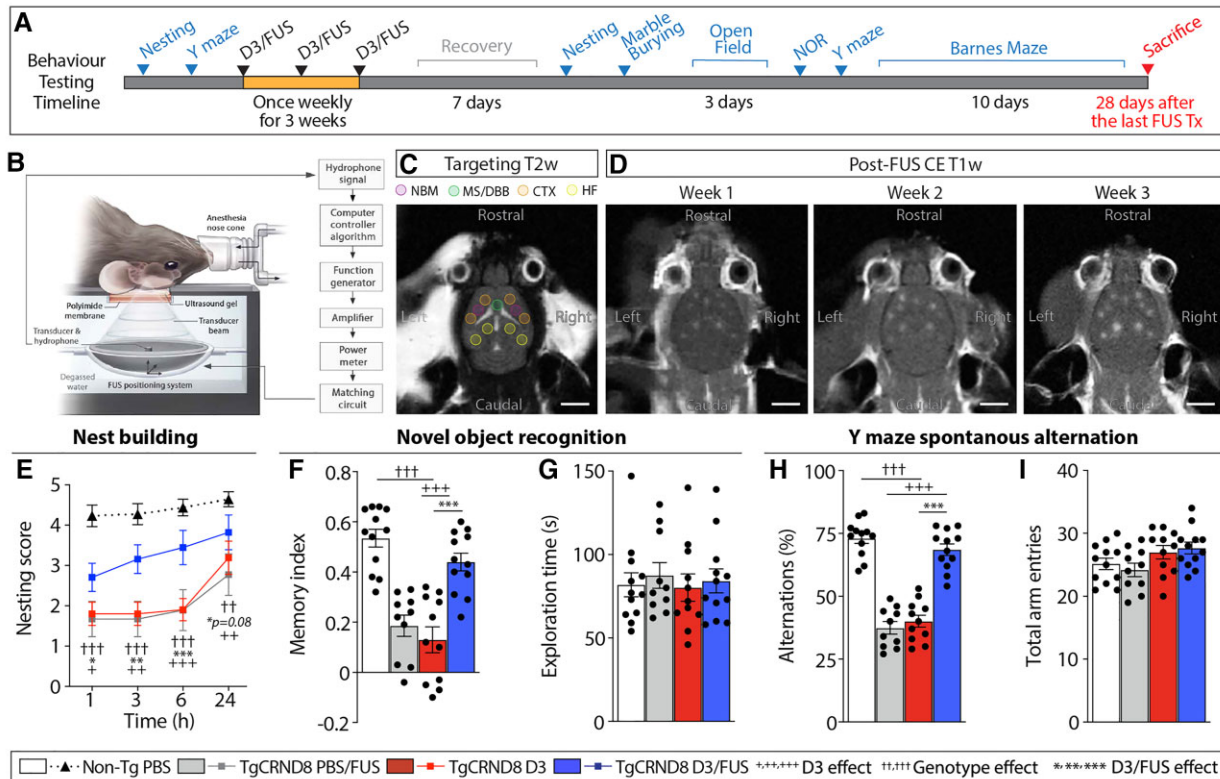


Figure 1 MRigFUS-mediated delivery of D3 in TgCRND8 mice. (A) Mice were treated once weekly for 3 weeks, then tested on a variety of behavioural tasks. (B) Focused ultrasound experimental setup.²¹ (C) Neuroanatomical regions of interests (coloured circles) were selected on T₂-weighted MRI. (D) BBB permeability in corresponding FUS-targeted areas was visualized over consecutive weeks on T₁-weighted MRI following the influx of a gadolinium-based MRI contrast agent. (E) D3 and PBS/FUS-treated TgCRND8 mice exhibited deficits in nest building activity, which was improved by D3/FUS treatment. (F) TgCRND8 treated with D3/FUS displayed improved reference memory performance in the novel object recognition task relative to PBS/FUS and D3-treated TgCRND8 mice. (G) Total exploration time for both familiar and novel objects was similar across experimental groups. (H) In the Y maze, D3/FUS was the only treatment to prevent deficits in spontaneous alternation in TgCRND8 mice. (I) Total arm entries were comparable across treatment conditions. Scale bars in C and D = 5 mm. Statistics: (E) Repeated measures and (F–I) one-way ANOVA with Holm-Sidak *post hoc* test. Significance: †*P* < 0.05; ††,†††*P* < 0.01, ††††,†††††*P* < 0.001. †Comparison of D3-treated TgCRND8 mice with PBS-treated non-Tg mice (genotype effect). †Comparison of PBS/FUS-treated with D3/FUS-treated TgCRND8 mice (D3 effect). *Comparison of D3-treated with D3/FUS-treated TgCRND8 mice (D3/FUS effect). Data represent means ± SEM; *n* = 10–12 per group.

and cortex, with regional differences in fibre densities (Fig. 4A and Supplementary Figs 7 and 8). In the CA1 and CA3 subfields of the hippocampus, the most notable loss of fibres in TgCRND8 mice appeared in the stratum radiatum and stratum lacunosum-moleculare (Fig. 4A and Supplementary Fig. 7). In the dentate gyrus, decreased fibre innervation was most prominent in the molecular layer (Supplementary Fig. 7). D3/FUS-treated mice exhibited increased cholinergic fibre density (Fig. 4A and Supplementary Fig. 7). TgCRND8 mice also displayed a significant decrease of ChAT+ fibre density in the frontal (Fig. 4A), parietal and entorhinal (Supplementary Fig. 8) cortices, which were increased following D3/FUS treatment. Overall, these findings demonstrate that TrkA stimulation is sufficient to rescue the degeneration and maintain the phenotype of BFCNs in TgCRND8 mice.

D3/FUS promotes cholinergic function in TgCRND8 mice

Next, we investigated whether anatomical changes at the level of the soma and terminal networks, as well as the functional upregulation of ChAT activity, led to enhanced cholinergic tone as measured by basal and potassium-induced ACh release in hippocampal and cortical slices (Fig. 4B). Potassium chloride

depolarization increased the release of ¹⁴C-ACh from brain slices. Potassium-induced ACh release was higher in D3/FUS treated slices compared to D3 or PBS/FUS-treated slices (Fig. 4B), suggesting that cholinergic tone was enhanced following D3/FUS in TgCRND8 mice. Regional analysis of evoked ACh release revealed similar trends in the hippocampus and several cortical areas (Fig. 4B). Consistent with increased ChAT activity (Fig. 3G), the levels of hippocampal and cortical tissue ACh content were significantly higher in D3/FUS-treated TgCRND8 compared to D3 and PBS/FUS-treated controls (Fig. 4C). Moreover, increased hippocampal and cortical AChE enzymatic activities were observed in D3/FUS-treated animals (Fig. 4D). Together, these findings demonstrate increased hippocampal and cortical cholinergic function as a result of D3/FUS treatment. Adequate levels of ACh synthesis and release serve to maintain cholinergic neurotransmission required for cognitive function.

D3/FUS stimulates hippocampal neurogenesis in TgCRND8 mice

The innervation of the hippocampus by medial septum cholinergic neurons promotes the proliferation and survival of hippocampal neural progenitor cells.³⁷ Newborn neurons of the dentate gyrus

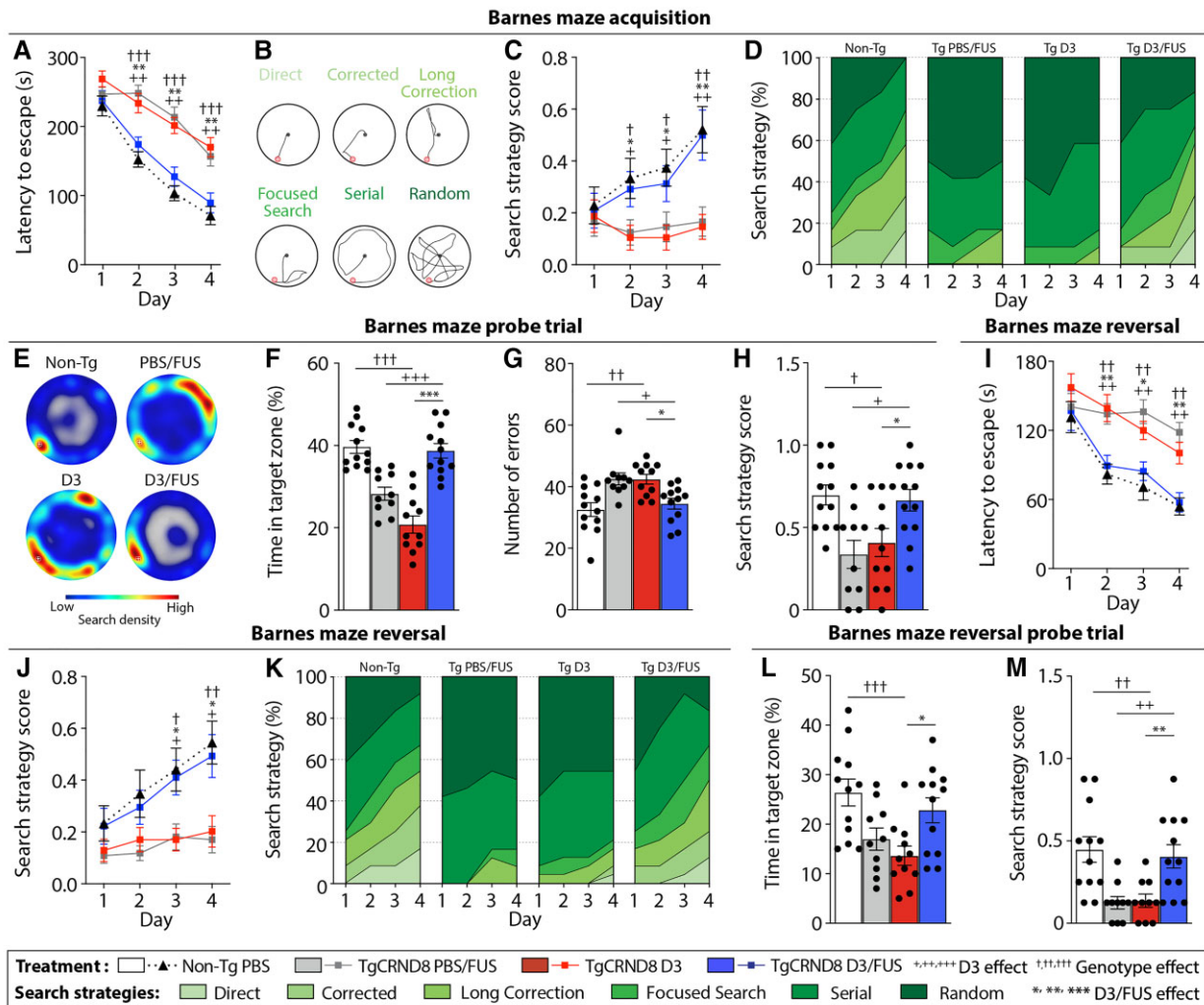


Figure 2 MRIgFUS-mediated delivery of D3 promotes spatial memory and cognitive flexibility in TgCRND8 mice. In the Barnes maze, D3/FUS enhanced spatial navigation in TgCRND8 mice relative to PBS/FUS and D3-treated TgCRND8 controls. (A) TgCRND8 mice demonstrated a slower learning curve relative to non-Tg mice, unless treated with D3/FUS. (B) Search strategies used by mice in the Barnes maze were classified. (C and D) Similar to non-Tg controls, D3/FUS-treated TgCRND8 mice used spatially-dependent search strategies to locate the escape box. (E–H) Performance in the probe test was improved by D3/FUS treatment, reflecting memory retention. This was demonstrated by (E) higher search density at the previous location of the escape box, (F) more time spent near the target hole in the absence of the escape box, (G) fewer entries in non-target holes (errors) and (H) higher search strategy scores of D3/FUS-treated TgCRND8 mice relative to PBS/FUS and D3-treated controls. (I–K) Barnes maze reversal learning, with the target hole re-located 180° from the original position, was improved by D3/FUS treatment in TgCRND8 mice. (I) Relative to PBS/FUS and D3-treated TgCRND8 mice, non-Tg mice and D3/FUS-treated TgCRND8 mice demonstrated faster escape latency, (J) better spatially-dependent navigation as demonstrated by higher search strategy scores and (K) percentage of spatial strategies used across trial days. (L and M) Performance in the reversal probe test was improved in TgCRND8 mice following D3/FUS treatment, with (L) more time spent in the target zone and (M) higher search strategy score relative to D3-treated TgCRND8 mice. Statistics: (A, C, I and J) Repeated measures and (F–H, L and M) one-way ANOVA with Holm-Sidak post hoc test. Significance: †,††P < 0.05; †††,††††P < 0.01, ††††,†††††P < 0.001. †Comparison of D3-treated TgCRND8 mice with PBS-treated non-Tg mice (genotype effect). *Comparison of PBS/FUS-treated with D3/FUS-treated TgCRND8 mice (D3 effect). **Comparison of D3-treated with D3/FUS-treated TgCRND8 mice (D3/FUS effect). Data represent means ± SEM; n = 10–12 per group.

continuously integrate into the hippocampal circuitry, contributing to learning and memory.³⁸ Thus, we evaluated hippocampal neurogenesis as another potential contributor to behavioural improvement following D3/FUS treatment.

To evaluate proliferative activity in the dentate gyrus, mice were injected with the thymidine analogue BrdU, 3, 4 and 5 days after the last treatment (Fig. 5A). Twenty-four hours later, BrdU incorporation was quantified in the dentate gyrus (Fig. 5A and B). D3/FUS increased the total number of BrdU+ cells in TgCRND8 mice relative to PBS/FUS, D3 and PBS-treated controls (Fig. 5C). To evaluate the proportion of proliferating cells that differentiated into neurons, cells

in the dentate gyrus were also analysed for co-expression of BrdU and the immature neuronal marker, DCX (Fig. 5D). Consistent with previous reports in TgCRND8 mice, there were fewer BrdU+/DCX+ cells in TgCRND8 mice compared to age-matched non-Tg controls;³⁹ this deficit was restored by D3/FUS relative to PBS/FUS, D3 and PBS-treated controls (Fig. 5D). It is worth noting that FUS alone also increased newborn neuron proliferation as previously reported,^{40,41} but to a lesser extent than D3/FUS (Fig. 5C and D). Newborn neurons are known to migrate into the granule cell layer during the first 4 weeks prior to functional integration into pre-existing circuits.³⁸ Here, the relative proportion of BrdU+ cells in

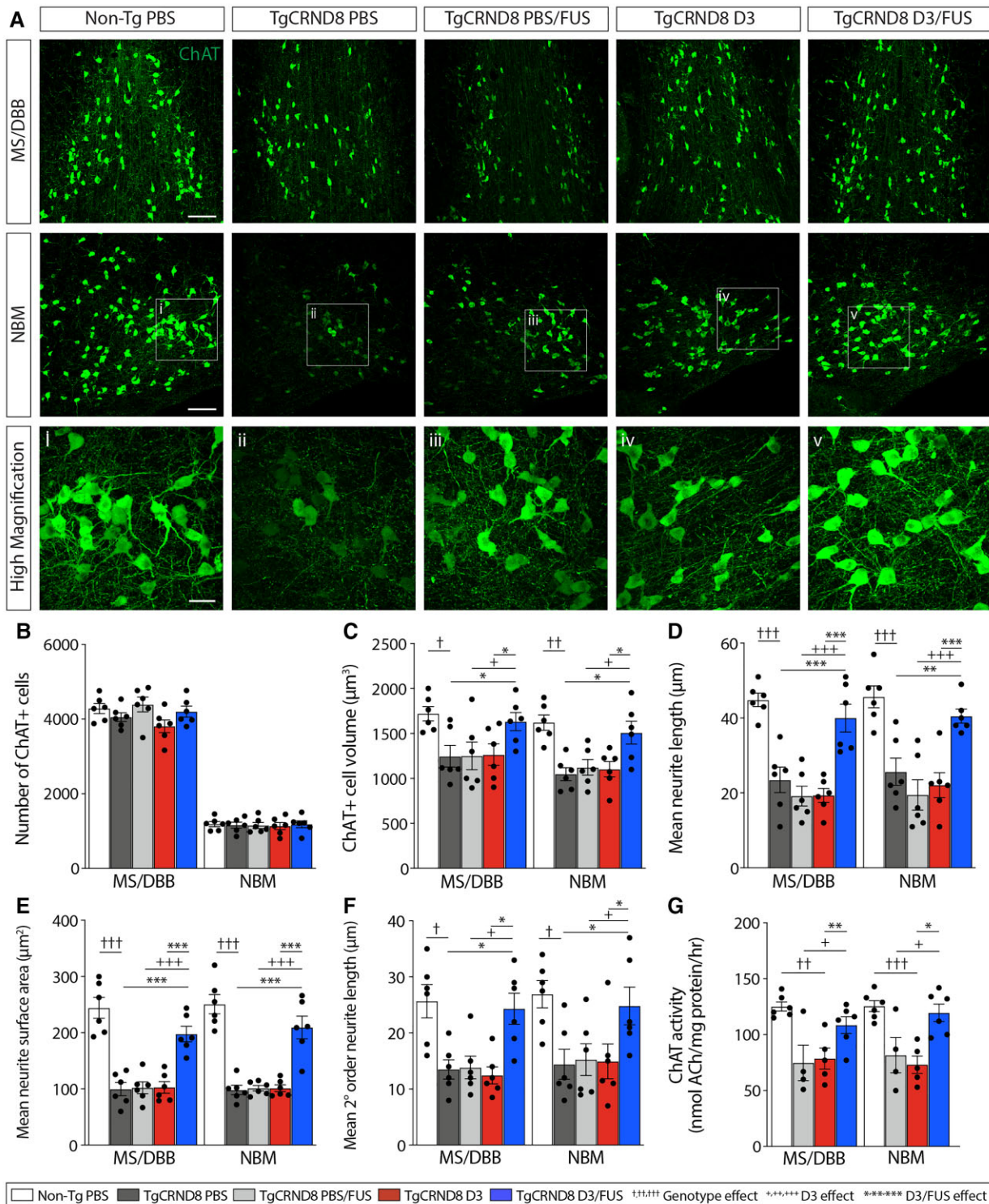


Figure 3 Repeated MRIgFUS delivery of D3 improves basal forebrain cholinergic neuron structural integrity and function in TgCRND8 mice. (A) Representative confocal images from non-Tg PBS, TgCRND8 PBS, PBS/FUS, D3 or D3/FUS-treated mice, show ChAT+ neurons in the MS/DBB and NBM. (B) Relative to non-TgCRND8, all groups of TgCRND8 mice had a comparable number of ChAT+ BFCNs. (C) Soma size, (D) mean neurite length, (E) total surface area and (F) branching complexity were decreased in ChAT+ BFCNs of PBS-treated TgCRND8 mice compared to non-Tg littermates, and increased with D3/FUS treatment. (G) ChAT enzyme activity was enhanced by D3/FUS in TgCRND8 mice and comparable to non-Tg levels. Scale bars in A = 100 μm; i–v = 30 μm. Statistics: one-way ANOVA with Holm-Sidak post hoc test. Significance: [†],^{††},^{†††}*P* < 0.05; ^{††††}*P* < 0.01, ^{†††††},^{††††††}*P* < 0.001. [†]Comparison of PBS-treated TgCRND8 mice with PBS-treated non-Tg mice (genotype effect). ^{*}Comparison of PBS/FUS-treated with D3/FUS-treated TgCRND8 mice (D3 effect). ^{*}Comparison of PBS and D3-treated TgCRND8 mice with D3/FUS-treated TgCRND8 mice as shown (D3/FUS effect). Data represent means ± SEM; *n* = 4–6 per group.

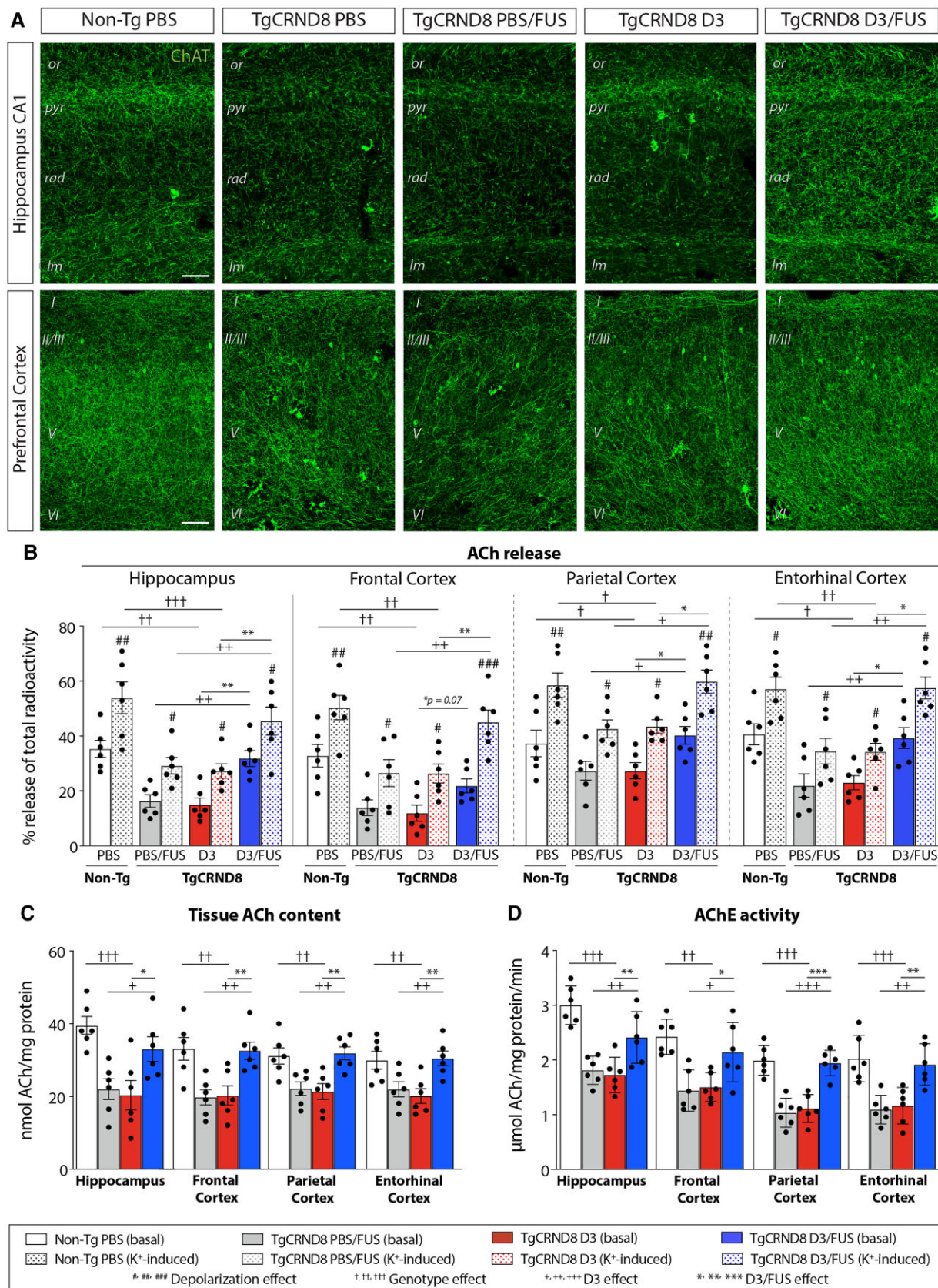


Figure 4 MRIgFUS-mediated delivery of D3 enhances cholinergic function in hippocampal and cortical areas. (A) Representative confocal images from non-Tg PBS, TgCRND8 PBS, PBS/FUS, D3 or D3/FUS-treated mice at 6.5 months of age show ChAT+ fibres in the hippocampus and prefrontal cortex. A decrease in ChAT+ fibre density in CA1 subfield of the hippocampus was apparent in PBS-treated TgCRND8 mice relative to non-Tg mice.

(Continued)

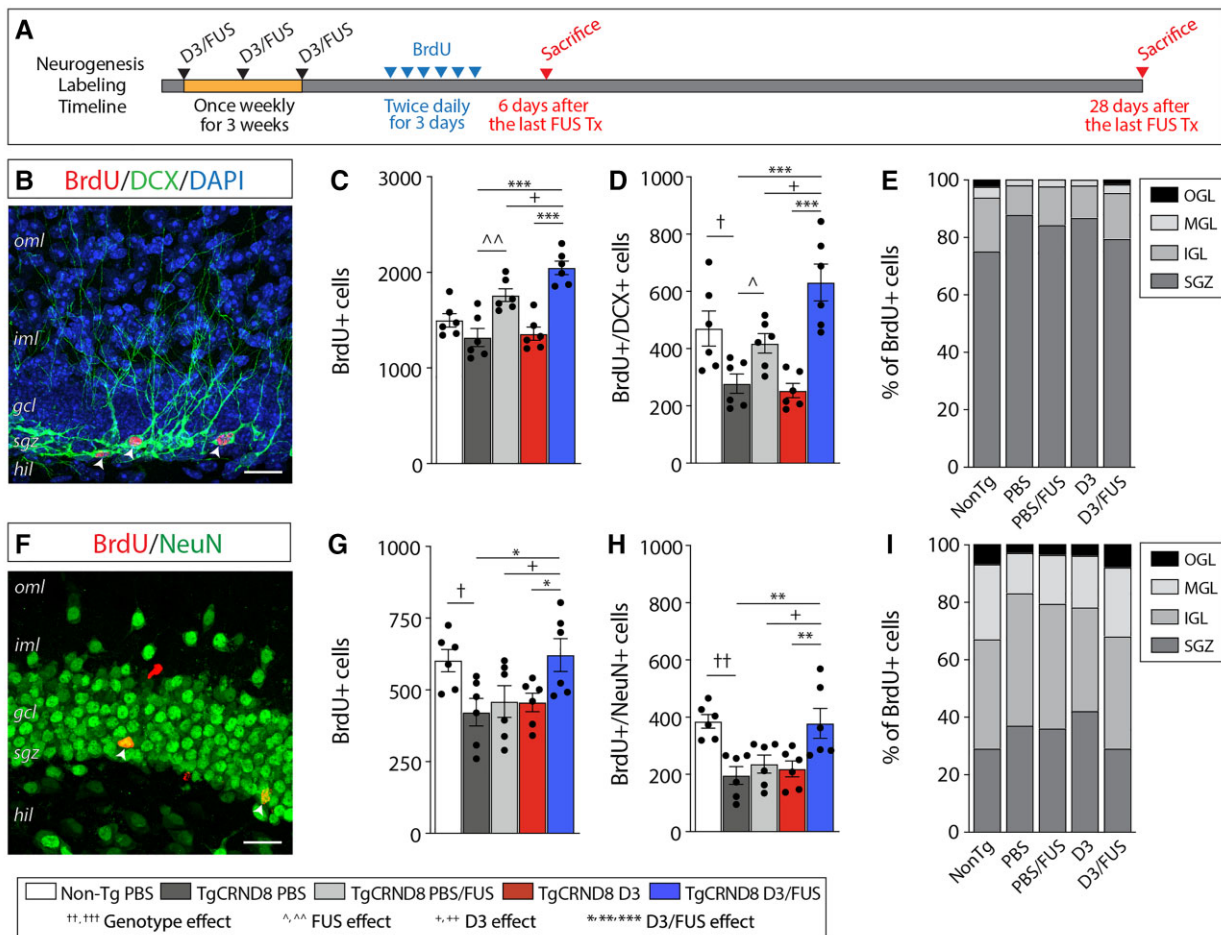


Figure 5 MRIgFUS BBB modulation combined with D3 delivery increases proliferation and survival of newborn neurons in TgCRND8 mice. (A) Following the last weekly treatment, separate cohorts of mice were injected with BrdU and sacrificed after 6 days and 28 days to label proliferating and surviving cells, respectively. (B) A representative confocal image of a BrdU (red), DCX (green), and DAPI (blue) labelled section 24 h after the last BrdU injection. (C) PBS/FUS-treated and D3/FUS-treated mice had more BrdU+ proliferating cells compared to PBS-treated TgCRND8 controls. (D) TgCRND8 mice had significantly fewer BrdU+ proliferating cells co-labelled with the immature neuronal marker DCX. This deficit was rescued by PBS/FUS and D3/FUS treatments. (E) Neuronal migration, as measured by the distribution of BrdU-labelled cells within the granule cell layer was impaired in TgCRND8 mice, and restored following D3/FUS treatment. (F) A representative confocal image of a BrdU (red) and NeuN (green) labelled section 28 days after the last treatment. (G) There was a significant genotype deficit in the number of surviving BrdU+ cells, (H) BrdU+ cells co-labelled with the mature neuronal marker NeuN, and (I) migration into the granule cell layer, which were increased in D3/FUS-treated mice. Statistics: (C–E, G–I) one-way ANOVA with Holm-Sidak post hoc test. Significance: $^{+,*}$ $p < 0.05$; **,* $p < 0.01$, *** $p < 0.001$; $^{+}$ Comparison of PBS-treated non-Tg mice with PBS-treated TgCRND8 mice (genotype effect); $^{^}$ Comparison of PBS-treated TgCRND8 mice with PBS/FUS-treated TgCRND8 mice (FUS effect); * Comparison of PBS/FUS-treated with D3/FUS-treated TgCRND8 mice (D3 effect). * Comparison of PBS and D3-treated TgCRND8 mice with D3/FUS-treated TgCRND8 mice as shown (D3/FUS effect). Data represent means \pm SEM; $n = 6$ per group. oml = outer molecular layer; iml = inner molecular layer; gcl = granule cell layer; sgz = subgranular zone; hil = hilus; igl = inner granule layer; mgl = middle granule layer; ogl = outer granule layer.

burden. D3/FUS treatment in TgCRND8 mice restored performance on tasks related to cognitive domains affected in Alzheimer's disease, including recognition memory, working memory, spatial learning and reference memory, cognitive flexibility and activities of daily living.⁴⁶ Administration of D3 or mutant NGF with reduced binding affinity to p75^{NTR} in transgenic models of amyloidosis, either prior to or at the onset of cognitive impairment and amyloid- β deposition, exerted neuroprotective effects, decreased brain amyloid- β levels and prevented memory deficits.^{12,20,47} To our knowledge, our study represents the first time TrkA-mediated bioeffects have been harnessed to improve cognition in the context of well-established behavioural deficits, amyloid- β plaque pathology and cholinergic dysfunction, similar to a prospective clinical condition.

We demonstrate that selective TrkA stimulation can promote neuronal function in the presence of Alzheimer's disease-related neurotrophic signalling deficits, which may render native NGF ineffective. The TrkA-specific ligand D3 promoted neuroprotection even in the presence of an imbalance between TrkA and p75^{NTR} expression in TgCRND8 mice,²¹ similar to Alzheimer's disease.¹⁶ Since TrkA expression is downregulated, native NGF may favour binding to p75^{NTR} over TrkA, leading to deficits in TrkA-mediated signalling and the selective vulnerability of BFCNs.¹⁷ In support of this hypothesis, we previously showed that native NGF failed to promote TrkA signalling in TgCRND8 mice.²¹ Native NGF also failed to restore cognition in hAPP-J20 transgenic mice, although NGF receptor levels remain to be characterized in this Alzheimer's disease model.²⁰

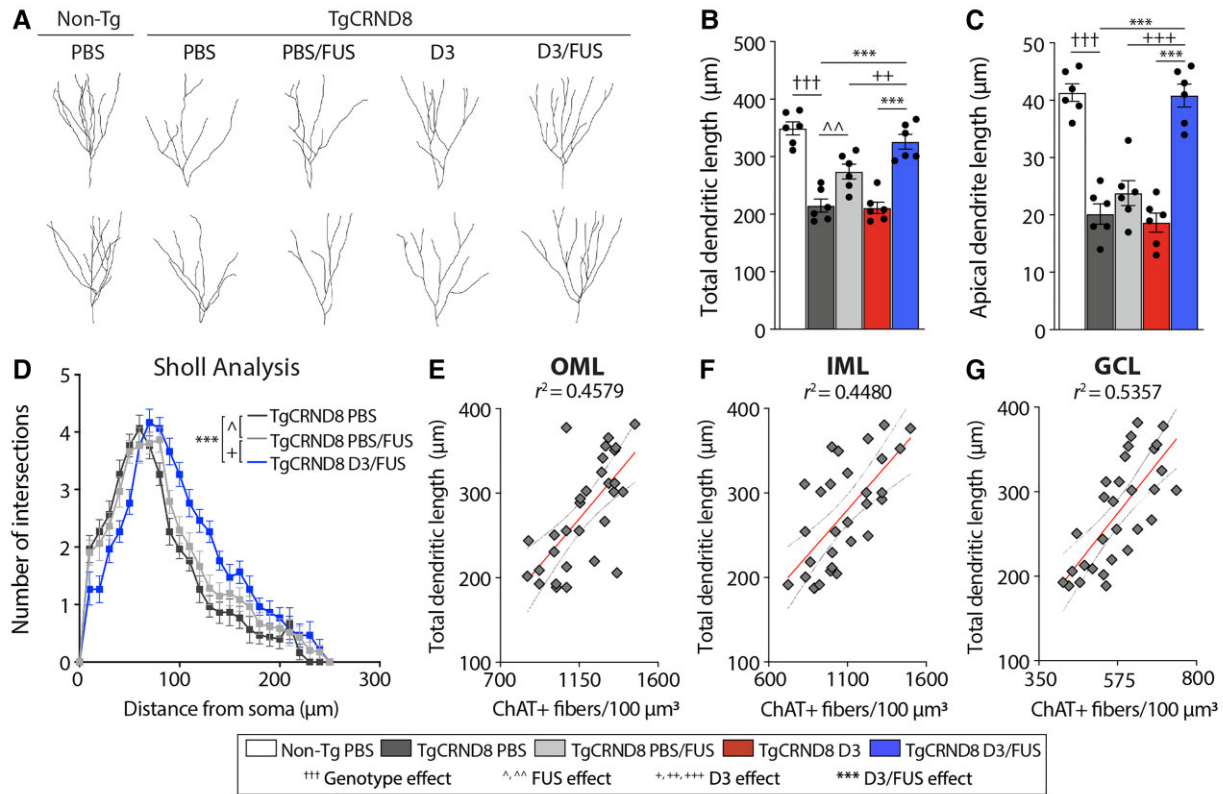


Figure 6 MRIgFUS-mediated delivery of D3 restores the dendritic complexity of newborn neurons in TgCRND8 mice. (A) Representative reconstructions of DCX+ cells across experimental groups to assess morphology of newborn granule neurons. (B) Decreased total dendritic length and (C) apical dendrite length in TgCRND8 mice was restored by D3/FUS treatment. (D) Sholl analysis of dendritic complexity demonstrated a left shift of the curve in PBS-treated TgCRND8 mice, which was normalized by D3/FUS treatment. (E) There was a positive correlation between total dendritic length of DCX+ fibres and ChAT+ fibre density in the outer molecular layer (OML), (F) inner molecular layer (IML) and (G) granule cell layer (GCL) subregions of the dentate gyrus. Scale bars = 30 μm . Statistics: (B and C) one-way and (D) two-way ANOVA with Holm-Sidak *post hoc* test. (E–G) Linear regression analysis. Dashed lines indicate a 95% confidence interval. Significance: *,[†] $P < 0.05$; [^],^{^^} $P < 0.01$, ^{***},^{****},^{†††} $P < 0.001$; [†]Comparison of PBS-treated non-Tg mice with PBS-treated TgCRND8 mice (genotype effect). [^]Comparison of PBS-treated TgCRND8 mice with PBS/FUS-treated TgCRND8 mice (FUS effect). ^{*}Comparison of PBS/FUS-treated with D3/FUS-treated TgCRND8 mice (D3 effect). ^{*}Comparison of PBS and D3-treated TgCRND8 mice with D3/FUS-treated TgCRND8 mice as shown (D3/FUS effect). Data represent means \pm SEM; $n = 6$ per group.

One notable mechanism by which cholinergic input from the basal forebrain modulates hippocampal circuitry is neurogenesis. Considerable evidence supports a role for neurogenesis in Alzheimer's disease. Neurogenesis is impaired by amyloid- β deposition in TgCRND8 mice^{35,39} and other mouse models of Alzheimer's disease.³⁸ Alterations in hippocampal neurogenesis have also been described in Alzheimer's disease patients.⁴⁸ Our results suggest that stimulating cholinergic tone, via MRIgFUS delivery of D3, can stimulate survival of newborn neurons, which may contribute to improved learning and memory, even in a hostile brain environment with Alzheimer's disease pathology (Fig. 5). In this context, it is worth noting the role of amyloid- β attenuation on the neurogenic niche; that is, whether amyloid- β reduction following D3/FUS could alone promote neurogenesis, and thereby ameliorate deficits in neurogenesis-related behavioural tasks. Previous work in 7-month-old TgCRND8 mice demonstrated that scyllo-inositol, an amyloid- β anti-aggregation agent that halts its progression, did not impact the proliferation and survival of newborn neurons; whereas combination treatment with neotrofin, a purine derivative that induces BDNF and NGF expression, was sufficient to promote neurogenesis.³⁹ Neotrofin treatment alone also did not enhance neurogenesis, indicating that amyloid- β indeed negatively regulates neurogenesis in this transgenic model.³⁹ Overall, these

data support a mechanism whereby neurogenesis after D3/FUS treatment is improved by modulating amyloid pathology and neurotrophic support in combination. Thus, sustained TrkA activation in the earliest stages of Alzheimer's disease pathology may protect hippocampal neurons from death with disease progression.

The effects of MRIgFUS-mediated TrkA activation extend to potent anti-amyloidogenic actions that may slow cognitive decline. Four weeks after the last D3/FUS treatment, widespread reduction in amyloid plaque pathology and cholinergic dystrophic neurites surrounding plaques were observed in the MRIgFUS-targeted cortex and hippocampus (Fig. 7). Our results are consistent with the decreased amyloid- β load in the cortex and hippocampus reported after non-targeted intranasal delivery of an NGF mutant with lower affinity for p75^{NTR} than native NGF (and identical binding to TrkA) over a 21-day period,¹² further supporting the notion of TrkA-mediated modulation of amyloidosis. In contrast, systemic administration of a BBB-permeable p75^{NTR} antagonist, LM11A-31, did not change the total cortical area occupied by plaques,⁴⁹ suggesting that NGF/TrkA signalling is responsible for reduced amyloid- β pathology. One potential mechanism by which increased cholinergic tone may be neuroprotective against amyloid- β -induced toxicity is by shifting APP processing towards nonamyloidogenic cleavage.⁵⁰ Second, a role for TrkA-mediated

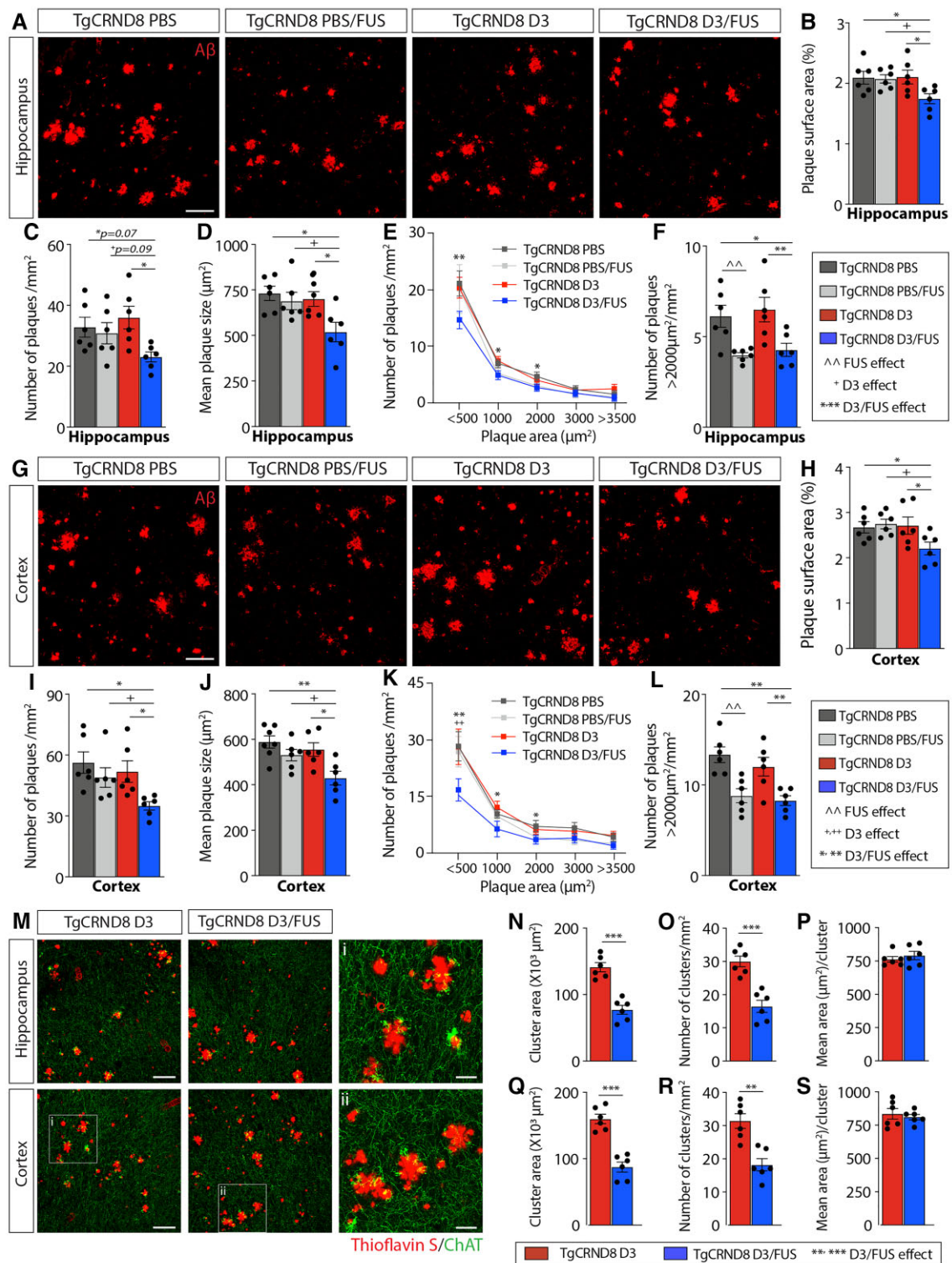


Figure 7 MRIgFUS-mediated delivery of D3 reduces amyloid plaque deposition and cholinergic dystrophic neurites in the cortex and hippocampus. (A) Representative confocal images from the hippocampus of PBS, PBS/FUS, D3 and D3/FUS-treated TgCRND8 mice stained for amyloid-β (red). (B) Total hippocampal surface area occupied by amyloid-β, (C) density of plaques and (D) mean plaque size were reduced in D3/FUS-treated mice relative to PBS, PBS/FUS and D3-treated mice. (E) A range of plaque sizes were decreased by D3/FUS treatment relative to PBS-treated controls. (F) The number of large plaques defined by an area >2000 μm² were reduced in PBS/FUS and D3/FUS-treated mice. (G) Representative amyloid-β staining from cortical brain sections. (H) D3/FUS treatment decreased cortical amyloid coverage, (I) density of plaques, and (J) mean plaque size. (K) A range of plaques sizes decreased by D3/FUS treatment relative to PBS-treated controls. (L) PBS/FUS treatment preferentially reduced the number of large plaques. (M) Representative confocal images of ChAT-immunostained dystrophic neurites (green) surrounding plaques labelled with Thioflavin S (red). (N) D3/FUS treatment decreased the total hippocampal area occupied by clusters of dystrophic neurites and (O) number of clusters, (P) but not the

(Continued)

amyloid- β clearance by microglia has been proposed.^{12,51} Third, transient BBB permeability induced by the interaction of ultrasound and microbubbles has been shown to reduce amyloid- β pathology in APP-overexpressing mice,^{40,52,53} albeit by incompletely understood clearance pathways. One underlying mechanism is increased internalization and degradation of amyloid- β by microglia that become activated in response to BBB modulation.^{52,53} Here, MRIgFUS treatment shifted the distribution of plaque size toward smaller plaques (Fig. 7E and K), with the total plaque area remaining unaffected (Fig. 7B and H). These findings are consistent with clearance of amyloid- β by microglia preventing further plaque growth. However, the reduction in amyloid- β pathology following MRIgFUS alone was not sufficient to improve performance in cognitive tasks (Fig. 1). In combination, factors such as cholinergic modulation of APP processing, and amyloid- β clearance by microglia as a result of direct TrkA stimulation and/or FUS-induced BBB permeability, may contribute to the overall reduction in amyloid- β pathology following D3/FUS treatment.

It is important to consider the overall contribution of amyloid- β reduction to neuronal and cognitive improvement. D3 selectively engages TrkA, a receptor widely accepted to be preferentially and highly expressed on cholinergic neurons,¹¹ supporting the hypothesis that it is trophic support provided to cholinergic neurons that ultimately drives the reduction of amyloid load. This interpretation is also consistent with the potent anti-amyloidogenic effects of cholinergic-related treatment in preclinical models of Alzheimer's disease.⁵⁰ Positive feedback could occur with amyloid- β reduction representing a means of reinforcing and strengthening cholinergic terminals. However, amyloid- β -directed interventions, including those that entirely halt amyloid- β accumulation, serve to slow down and/or prevent further neuronal degeneration, rather than rescue atrophy as observed in this study. Additionally, while D3/FUS treatment does indeed reduce amyloid plaque load, it does not halt the progression of amyloid- β pathology to baseline levels observed in 5-month-old TgCRND8 mice (Supplementary Fig. 1). Thus, it is unlikely that the lower levels of amyloid- β following D3/FUS is the main effect driving improvements in neuronal structure, function and downstream cognition, matched to non-Tg levels. Emerging evidence in Alzheimer's disease patients also implicates a role for NGF/TrkA signalling, cholinergic neurotransmission and neurogenesis in neuronal resilience to Alzheimer's disease pathology,^{54–56} supporting the promise of D3/FUS treatment as a neuroprotective therapy beyond its effects on amyloid- β levels. Collectively, we interpret our results to support the notion that D3/FUS confers neuroprotection in the presence of established amyloid pathology, and that sustained treatment reduces amyloid- β burden, to positively impact neuronal and cognitive function.

MRIgFUS offers several advantages as a drug delivery modality to achieve NGF-associated bioeffects in the brain. In contrast to current clinical trials that rely on invasive intracranial procedures, MRIgFUS is applied transcranially, thereby minimizing the risk of surgery-related complications. Drug delivery to several brain regions requires multiple injection sites, whereas multiple focal points can be created simultaneously using MRIgFUS, further

mitigating technical challenges and improving safety. Furthermore, MRIgFUS-induced BBB permeability, as a proxy for drug delivery, can be visualized by gadolinium leakage at targeted sites immediately after sonication. These features are particularly important in light of recent evidence from NGF clinical trials that report inaccurate targeting and inefficient spread of AAV2-NGF delivery by stereotaxic injection.¹⁴ Emerging evidence also suggests that FUS-mediated BBB permeability may modulate neuronal plasticity and reduce amyloid- β pathology, further supporting its clinical potential.^{40,41,52,53,57,58} Relevant to this work, we previously demonstrated that MRIgFUS alone increased NGF levels within 90 min post-sonication, concurrent with D3 delivery in 6-month-old TgCRND8 mice.²¹ Consistent with previous findings, following MRIgFUS alone, we also demonstrate an increase in neural progenitor cell proliferation and the dendritic complexity of newborn neurons,^{40,41,57} yet not newborn neuron survival (Fig. 5). Amyloid- β attenuation following FUS follows a similar trend; the effect size is greater immediately after sonication, but returns to baseline over time.⁵⁸ Overall, these results indicate that the effects of FUS alone are likely transient, and perhaps less pronounced in the hostile microenvironment generated by amyloid- β pathology. Future work will be required to optimize treatment frequency in order to harness the beneficial effects of FUS-induced BBB permeability.

An important safety consideration for clinical translation is whether MRIgFUS BBB modulation itself impacts behavioural and cognitive function in Alzheimer's disease patients. To date, behavioural effects of MRIgFUS BBB permeability have sparingly addressed in preclinical models with mid-late stage amyloid- β pathology. We demonstrate that MRIgFUS alone does not adversely affect recognition memory in the novel object recognition task (Fig. 1F) or spatial working memory using the spontaneous alternation Y maze test (Fig. 1H), consistent with findings in APP23 transgenic mice with early-stage pathology and no underlying impairment in these tasks.⁵³ We also report comparable spatial learning and memory in the Barnes maze relative to untreated TgCRND8 mice (Fig. 2A–H). Repeated ultrasound treatment improved spatial learning and memory in young APP23 transgenic mice as assessed in the active place avoidance test,⁵³ but it may be insufficient to rescue cognitive deficits as a result of more advanced neuropathology, as seen in 6-month-old TgCRND8 mice in our study. Burgess *et al.* report improved performance in the reference memory version of the Y maze in older 8-month-old TgCRND8 following MRIgFUS.⁴⁰ However, spatial mapping demands in the active place avoidance test and Y maze are significantly lower than in the Barnes maze, and thus more likely to yield changes in behaviour. Nevertheless, unimpaired performance in the Barnes maze after MRIgFUS treatment underscores the fact that spatial learning and memory is not adversely affected.

We also present data on tasks requiring substantial attentional effort; another cognitive domain severely affected in Alzheimer's disease patients and modulated by cholinergic tone.⁵⁹ Cognitive flexibility was unaltered by repeated MRIgFUS in the Barnes maze (Fig. 2I–M). Attention deficits in Alzheimer's disease patients are also associated with impaired performance on activities of daily

Figure 7 Continued

mean ChAT+ area per cluster relative to D3-treated controls. (Q) Quantitative analysis in the cortex revealed the same trend in cluster area, (R) cluster number (S) and mean area per cluster. Scale bars in A, G and M = 100 μ m; i and ii = 30 μ m. Statistics: (B–D, F, H–J and L) one-way and (E and K) two-way ANOVA with Holm-Sidak *post hoc* test; (N–P and Q–S) unpaired Student's *t*-test. Significance: * $P < 0.05$; ** $P < 0.01$; *** $P < 0.001$. ^Comparison of PBS-treated mice with PBS/FUS-treated TgCRND8 mice (FUS effect). *Comparison of PBS/FUS-treated with D3/FUS-treated TgCRND8 mice (D3 effect). ^Comparison of PBS or D3-treated TgCRND8 mice with D3/FUS-treated TgCRND8 mice as shown (D3/FUS effect). Data are presented as mean \pm SEM; $n = 6$ per group.

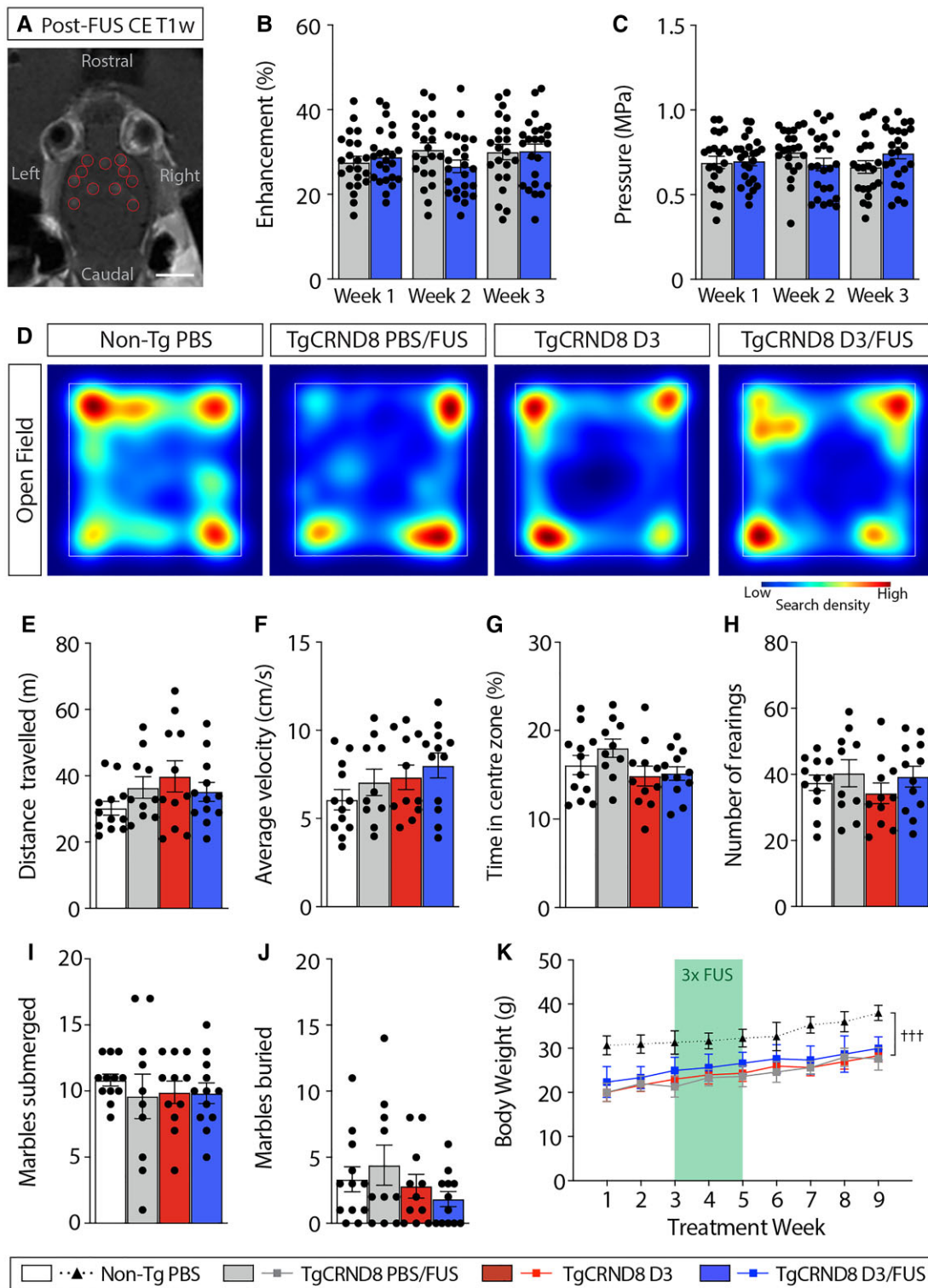


Figure 8 Locomotor function, anxiety-like behaviour and body weight are not affected following MRIgFUS-mediated delivery of D3. (A) BBB permeability was visualized by the influx of a gadolinium-based MRI contrast agent in sonicated focal spots (red circles). (B) The relative contrast enhancement and (C) sonication pressure were comparable between PBS/FUS and D3/FUS-treated mice, and across repeated sonications. (D) Heat map of general locomotor activity in the open field test. (E) Motor function measured by total distance travelled and (F) average velocity over a 10 min trial was similar across experimental groups. (G) No differences in anxiety-related behaviours were observed across treatment conditions, including time spent in the centre zone and (H) and number of rearing events. (I) Performance in the marble burying test was not impaired; the number of marbles submerged and (J) marbles buried were comparable in all conditions. (K) TgCRND8 mice weighed less than non-Tg mice throughout the study and body weight was not affected by repeated PBS/FUS, D3 or D3/FUS treatment. Scale bar in A = 5 mm. Statistics: (B, C and K) Repeated measures or (E–J) one-way ANOVA with Holm-Sidak post hoc test. Significance: †††*P* < 0.001. †Comparison of D3/FUS-treated TgCRND8 mice with PBS-treated non-Tg mice (genotype effect). Data represent means ± SEM; (B and C) *n* = 22–24 per group, (E–K) *n* = 10–12 per group.

living.⁵⁹ Here, there was no difference in nest construction, as a measure of daily living activity, after MRIgFUS treatment. MRIgFUS did not affect general locomotion and anxiety-related behaviour during the open field test (Fig. 8D–H) and anxiety-like behaviour in the marble burying task (Fig. 8I and J). These results are consistent with other preclinical studies that report increased BBB permeability in the absence of oedema, neuronal damage and haemorrhage using similar sonication parameters and real-time acoustic feedback control.^{40,58,60} Repeated MRIgFUS-BBB modulation is well-tolerated in Alzheimer's disease patients, further supporting the safety of this drug delivery modality.^{61,62} Our results show that MRIgFUS does not negatively impact cognitive outcomes when applied in a preclinical model with significant cognitive decline as a consequence of Alzheimer's disease pathogenesis, expanding on the body of evidence that supports the safety of MRIgFUS in the Alzheimer's disease brain.

At this stage, there remain several hurdles before TrkA activation combined with MRIgFUS can be realized in therapeutic applications for Alzheimer's disease. First, current amyloidosis models do not recapitulate the full spectrum of Alzheimer's disease pathology; the effect of MRIgFUS delivery of D3 on other Alzheimer's disease-related pathologies such as tau pathology and frank neuronal death is still to be determined. Bellucci *et al.* previously reported BFCN loss in 7-month-old TgCRND8 mice,³¹ but this was not observed in our study. Nevertheless, we demonstrate substantial cholinergic downregulation, reduced terminal fields, size and phenotype of BFCNs, which impact steady-state cholinergic tone and cognitive decline. Thus, the TgCRND8 model is an Alzheimer's disease-relevant preclinical model to evaluate cholinergic interventions such as D3/FUS treatment.

Second, clinical trials with NGF-based therapies have reported side effects such as pain and weight loss.⁶³ Here, systemic delivery of D3 did not reduce body weight over the course of treatment and 1-month follow-up period (Fig. 8K). Moreover, locomotion was unaffected in D3 and D3/FUS-treated mice in the open field test (Fig. 8D–F). These findings suggest that systemic D3 administration is well-tolerated. However, specific pain modality testing was not included in the current study. Future work will be necessary to determine potential sensitivity to pain and establish an effective dose below that threshold, if present.

Third, treatment with a TrkA ligand must take into account the integrity of the individual's cholinergic system. Preclinical evidence indicates that the effect of TrkA activation on cognition is largely dependent on the brain microenvironment, including age and disease state. While D3 administration improved spatial learning and memory in aged rats and in APP transgenic mice,^{19,20} deficits in spatial memory performance resulted in wild-type, healthy rodents^{20,64}—likewise for NGF.^{65–67} Treatment with NGF or selective TrkA agonists in APP transgenic models without cholinergic degeneration still supported BFCN function and spatial memory,^{12,20,47} suggesting that under pathological conditions such as cerebral amyloid burden where TrkA signalling is continuously negatively regulated, TrkA stimulation does not negatively impact intact neuronal networks. Personalized therapy with consideration for underlying cholinergic deficits will inform dosing, treatment frequency, and FUS targeting of affected brain regions. Clinical assessment of the BFCNs may be achieved by PET imaging with Trk-specific radiotracers⁶⁸ or cholinergic-targeted ligands such as ¹¹C-MP4A, which binds AChE.⁶⁹ *In vivo* imaging of cortical cholinergic terminals with ¹¹C-MP4A-PET in MCI patients was found to predict the behavioural response to cholinergic pharmacotherapy, supporting its use clinically.⁶⁹

The downregulation of TrkA in cholinergic neurons that undergo selective degeneration in Alzheimer's disease highlights an important therapeutic role for TrkA-specific agonists. Our findings provide compelling evidence that selective TrkA stimulation, using MRIgFUS as a clinically feasible drug delivery platform, can protect against amyloid- β -driven neurodegeneration, including cholinergic deficits and reduced hippocampal neurogenesis, thereby offering a potentially powerful disease-modifying treatment strategy to improve cognitive function in Alzheimer's disease.

Acknowledgements

We acknowledge Drs Paul Fraser, David Westaway, and Peter St George-Hyslop for supplying breeding pairs of TgCRND8 mice; Kristina Mikloska and Dr. Sheng-Kai Wu for MRIgFUS expertise; Shawna Rideout-Gros, Viva Chan and Melissa Theodore for animal care; Hang Yu Lin for illustrations; Dr Christopher Morrone for helpful consultation on behavioural testing and analyses.

Funding

This work was supported by the Canadian Institutes of Health Research (FRN-93603 to I.A., FDN-154272 to K.H.), Weston Brain Institute (TR130117 to I.A.), National Institute of Biomedical Imaging and Bioengineering (RO1-EB003268 to K.H.), Canadian Consortium on Neurodegeneration in Aging (to H.U.S.), FDC Foundation, WB Family Foundaton, Gerald and Carla Connor. This research was undertaken, in part, thanks to funding from the Canada Research Chairs Program (I.A., Tier 1 CRC in Brain Repair and Regeneration) and the Temerty Chair in Focused Ultrasound Research at Sunnybrook Health Sciences Centre. K.X. was awarded a Frederick Banting and Charles Best Canada Graduate Scholarship (GSD-152271). R.H.K. received a Postdoctoral Fellowship from the Alzheimer Society of Canada (19-10).

Competing interests

K.H. is co-founder of FUS Instruments and inventor on several patents related to BBB modulation using ultrasound.

Supplementary material

Supplementary material is available at *Brain* online.

References

- Chen X-Q, Mobley WC. Exploring the pathogenesis of Alzheimer disease in basal forebrain cholinergic neurons: Converging insights from alternative hypotheses. *Front Neurosci.* 2019;13:446.
- Dubois B, Chupin M, Hampel H, *et al.* Donepezil decreases annual rate of hippocampal atrophy in suspected prodromal Alzheimer's disease. *Alzheimers Dement.* 2015;11:1041–1049.
- Cavedo E, Dubois B, Colliot O, *et al.* Reduced regional cortical thickness rate of change in donepezil-treated subjects with suspected prodromal Alzheimer's disease. *J Clin Psychiatry.* 2016;77:e1631–e1638.
- Cavedo E, Grothe MJ, Colliot O, *et al.* Reduced basal forebrain atrophy progression in a randomized donepezil trial in prodromal Alzheimer's disease. *Sci Rep.* 2017;7:11706.

5. Tuszynski MH, Thal L, Pay M, et al. A phase 1 clinical trial of nerve growth factor gene therapy for Alzheimer's disease. *Nat Med.* 2005;11:551–555.
6. Rafii MS, Tuszynski MH, Thomas RG, et al. Adeno-associated viral vector (Serotype 2)-nerve growth factor for patients with Alzheimer disease: A randomized clinical trial. *JAMA Neurol.* 2018;75:834–841.
7. Karami A, Eyjolfssdottir H, Vijayaraghavan S, et al. Changes in CSF cholinergic biomarkers in response to cell therapy with NGF in patients with Alzheimer's disease. *Alzheimers Dement.* 2015;11:1316–1328.
8. Eriksdotter-Jönhagen M, Linderöth B, Lind G, et al. Encapsulated cell biodelivery of nerve growth factor to the basal forebrain in patients with Alzheimer's disease. *Dement Geriatr Cogn Disord.* 2012;33:18–28.
9. Eyjolfssdottir H, Eriksdotter M, Linderöth B, et al. Targeted delivery of nerve growth factor to the cholinergic basal forebrain of Alzheimer's disease patients: application of a second-generation encapsulated cell biodelivery device. *Alzheimers Res Ther.* 2016;8:30.
10. Ferreira D, Westman E, Eyjolfssdottir H, et al. Brain changes in Alzheimer patients with implanted encapsulated cells releasing nerve growth factor. *J Alzheimers Dis.* 2015;43:1059–1072.
11. Cuello AC, Pentz R, Hall H. The brain NGF metabolic pathway in health and in Alzheimer's pathology. *Front Neurosci.* 2019;13:62.
12. Capsoni S, Malerba F, Carucci NM, et al. The chemokine CXCL12 mediates the anti-amyloidogenic action of painless human nerve growth factor. *Brain.* 2017;140:201–217.
13. Honig LS. Gene therapy in Alzheimer disease—it may be feasible, but will it be beneficial? *JAMA Neurol.* 2018;75:791–793.
14. Castle MJ, Baltanás FC, Kovacs I, Nagahara AH, Barba D, Tuszynski MH. Postmortem analysis in a clinical trial of AAV2-NGF gene therapy for Alzheimer's disease identifies a need for improved vector delivery. *Hum Gene Ther.* 2020;31:415–422.
15. Wahlberg LU, Lind G, Almqvist MP, et al. Targeted delivery of nerve growth factor via encapsulated cell biodelivery in Alzheimer disease: a technology platform for restorative neurosurgery. *J Neurosurg.* 2012;117:340–347.
16. Xhima K, Aubert I. The therapeutic potential of nerve growth factor combined with blood-brain barrier modulation by focused ultrasound for neurodegenerative disorders. *Neural Regen Res.* 2021;16:1783–1785.
17. Ginsberg SD, Che S, Wu J, Counts SE, Mufson EJ. Down regulation of trk but not p75NTR gene expression in single cholinergic basal forebrain neurons mark the progression of Alzheimer's disease. *J Neurochem.* 2006;97:475–487.
18. Maliartchouk S, Feng Y, Ivanisevic L, et al. A designed peptidomimetic agonistic ligand of TrkA nerve growth factor receptors. *Mol Pharmacol.* 2000;57:385–391.
19. Bruno MA, Clarke PBS, Seltzer A, et al. Long-lasting rescue of age-associated deficits in cognition and the CNS cholinergic phenotype by a partial agonist peptidomimetic ligand of TrkA. *J Neurosci.* 2004;24:8009–8018.
20. Aboukassim T, Tong X-K, Tse YC, et al. Ligand-dependent TrkA activity in brain differentially affects spatial learning and long-term memory. *Mol Pharmacol.* 2011;80:498–508.
21. Xhima K, Markham-Coultes K, Nedev H, et al. Focused ultrasound delivery of a selective TrkA agonist rescues cholinergic function in a mouse model of Alzheimer's disease. *Sci Adv.* 2020;6:eaax6646.
22. Xhima K, McMahon D, Ntiri E, Goubran M, Hynynen K, Aubert I. Intravenous and non-invasive drug delivery to the mouse basal forebrain using MRI-guided focused ultrasound. *Bio Protoc.* 2021;11:e4056.
23. Chishti MA, Yang DS, Janus C, et al. Early-onset amyloid deposition and cognitive deficits in transgenic mice expressing a double mutant form of amyloid precursor protein 695. *J Biol Chem.* 2001;276:21562–21570.
24. Nagy PM, Aubert I. Overexpression of the vesicular acetylcholine transporter increased acetylcholine release in the hippocampus. *Neuroscience.* 2012;218:1–11.
25. Thal DR, Rüb U, Orantes M, Braak H. Phases of A beta-deposition in the human brain and its relevance for the development of Alzheimer's disease. *Neurology.* 2002;58:1791–800.
26. Adalbert R, Nogradi A, Babetto E, et al. Severely dystrophic axons at amyloid plaques remain continuous and connected to viable cell bodies. *Brain.* 2009;132:402–416.
27. Kimura R, MacTavish D, Yang J, Westaway D, Jhamandas JH. Beta amyloid-induced depression of hippocampal long-term potentiation is mediated through the amylin receptor. *J Neurosci.* 2012;32:17401–17406.
28. Hamm V, Héraud C, Bott JB, et al. Differential contribution of APP metabolites to early cognitive deficits in a TgCRND8 mouse model of Alzheimer's disease. *Sci Adv.* 2017;3:e1601068.
29. Brautigam H, Steele JW, Westaway D, et al. The isotropic fractionator provides evidence for differential loss of hippocampal neurons in two mouse models of Alzheimer's disease. *Mol Neurodegener.* 2012;7:58.
30. Steele JW, Brautigam H, Short JA, et al. Early fear memory defects are associated with altered synaptic plasticity and molecular architecture in the TgCRND8 Alzheimer's disease mouse model. *J Comp Neurol.* 2014;522:2319–2335.
31. Bellucci A, Luccarini I, Scali C, et al. Cholinergic dysfunction, neuronal damage and axonal loss in TgCRND8 mice. *Neurobiol Dis.* 2006;23:260–272.
32. McKeever PM, Kim T, Hesketh AR, et al. Cholinergic neuron gene expression differences captured by translational profiling in a mouse model of Alzheimer's disease. *Neurobiol Aging.* 2017;57:104–119.
33. Proulx É, Fraser P, McLaurin J, Lambe EK. Impaired cholinergic excitation of prefrontal attention circuitry in the TgCRND8 model of Alzheimer's disease. *J Neurosci.* 2015;35:12779–12791.
34. Proulx É, Power SK, Oliver DK, Sargin D, McLaurin J, Lambe EK. Apamin improves prefrontal nicotinic impairment in mouse model of Alzheimer's disease. *Cereb Cortex.* 2020;30:563–574.
35. Maliszewska-Cyna E, Xhima K, Aubert I. A comparative study evaluating the impact of physical exercise on disease progression in a mouse model of Alzheimer's disease. *J Alzheimers Dis.* 2016;53:243–257.
36. Herring A, Ambrée O, Tomm M, et al. Environmental enrichment enhances cellular plasticity in transgenic mice with Alzheimer-like pathology. *Exp Neurol.* 2009;216:184–192.
37. Itou Y, Nochi R, Kuribayashi H, Saito Y, Hisatsune T. Cholinergic activation of hippocampal neural stem cells in aged dentate gyrus. *Hippocampus.* 2011;21:446–459.
38. Christian KM, Ming G-L, Song H. Adult neurogenesis and the dentate gyrus: Predicting function from form. *Behav Brain Res.* 2020;379:112346.
39. Morrone CD, Thomason LAM, Brown ME, Aubert I, McLaurin J. Effects of neurotrophic support and amyloid-targeted combined therapy on adult hippocampal neurogenesis in a transgenic model of Alzheimer's disease. *PLoS One.* 2016;11:e0165393.
40. Burgess A, Dubey S, Yeung S, et al. Alzheimer disease in a mouse model: MR imaging-guided focused ultrasound targeted to the hippocampus opens the blood-brain barrier and improves pathologic abnormalities and behaviour. *Radiology.* 2014;273:736–745.

41. Shin J, Kong C, Lee J, et al. Focused ultrasound-induced blood-brain barrier opening improves adult hippocampal neurogenesis and cognitive function in a cholinergic degeneration dementia rat model. *Alzheimers Res Ther.* 2019;11:110.
42. Llorens-Martín M, Jurado-Arjona J, Fuster-Matanzo A, Hernández F, Rábano A, Ávila J. Peripherally triggered and GSK-3 β -driven brain inflammation differentially skew adult hippocampal neurogenesis, behavioural pattern separation and microglial activation in response to ibuprofen. *Transl Psychiatry.* 2014;4:e463.
43. Petty BG, Cornblath DR, Adornato BT, et al. The effect of systemically administered recombinant human nerve growth factor in healthy human subjects. *Ann Neurol.* 1994;36:244–246.
44. Winkler J, Ramirez GA, Kuhn HG, et al. Reversible Schwann cell hyperplasia and sprouting of sensory and sympathetic neurites after intraventricular administration of nerve growth factor. *Ann Neurol.* 1997;41:82–93.
45. Hanna A, Horne P, Yager D, Eckman C, Eckman E, Janus C. Amyloid beta and impairment in multiple memory systems in older transgenic APP TgCRND8 mice. *Genes Brain Behav.* 2009;8:676–684.
46. McKhann GM, Knopman DS, Chertkow H, et al. The diagnosis of dementia due to Alzheimer's disease: recommendations from the National Institute on Aging-Alzheimer's Association workgroups on diagnostic guidelines for Alzheimer's disease. *Alzheimers Dement.* 2011;7:263–269.
47. Capsoni S, Marinelli S, Ceci M, et al. Intranasal 'painless' human Nerve Growth Factor slows amyloid neurodegeneration and prevents memory deficits in App X PS1 mice. *PLoS One.* 2012;7:e37555.
48. Moreno-Jiménez EP, Flor-García M, Terreros-Roncal J, et al. Adult hippocampal neurogenesis is abundant in neurologically healthy subjects and drops sharply in patients with Alzheimer's disease. *Nat Med.* 2019;25(4):554–560.
49. Simmons DA, Knowles JK, Belichenko NP, et al. A small molecule p75NTR ligand, LM11A-31, reverses cholinergic neurite dystrophy in Alzheimer's disease mouse models with mid- to late-stage disease progression. *PLoS One.* 2014;9(8):e102136.
50. Fisher A. Cholinergic modulation of amyloid precursor protein processing with emphasis on M1 muscarinic receptor: perspectives and challenges in treatment of Alzheimer's disease. *J Neurochem.* 2012;120(Suppl 1):22–33.
51. Rizzi C, Tiberi A, Giustizieri M, et al. NGF steers microglia toward a neuroprotective phenotype. *Glia.* 2018;66(7):1395–1416.
52. Jordão JF, Thévenot E, Markham-Coultes K, et al. Amyloid- β plaque reduction, endogenous antibody delivery and glial activation by brain-targeted, transcranial focused ultrasound. *Exp Neurol.* 2013;248:16–29.
53. Leinenga G, Götz J. Scanning ultrasound removes amyloid- β and restores memory in an Alzheimer's disease mouse model. *Sci Transl Med.* 2015;7(278):278ra33.
54. Mufson EJ, Mahady L, Waters D, et al. Hippocampal plasticity during the progression of Alzheimer's disease. *Neuroscience.* 2015;309:51–67.
55. Garibotto V, Tettamanti M, Marcone A, et al. Cholinergic activity correlates with reserve proxies in Alzheimer's disease. *Neurobiol Aging.* 2013;34:2694.e13–2694.e18.
56. Stern Y. Cognitive reserve in ageing and Alzheimer's disease. *Lancet Neurol.* 2012;11:1006–1012.
57. Scarcelli T, Jordão JF, O'Reilly MA, Ellens N, Hynynen K, Aubert I. Stimulation of hippocampal neurogenesis by transcranial focused ultrasound and microbubbles in adult mice. *Brain Stimul.* 2014;7:304–307.
58. Poon CT, Shah K, Lin C, et al. Time course of focused ultrasound effects on β -amyloid plaque pathology in the TgCRND8 mouse model of Alzheimer's disease. *Sci Rep.* 2018;8:14061.
59. Malhotra PA. Impairments of attention in Alzheimer's disease. *Curr Opin Psychol.* 2019;29:41–48.
60. O'Reilly MA, Hynynen K. Blood-brain barrier: real-time feedback-controlled focused ultrasound disruption by using an acoustic emissions-based controller. *Radiology.* 2012;263:96–106.
61. Lipsman N, Meng Y, Bethune AJ, et al. Blood-brain barrier opening in Alzheimer's disease using MR-guided focused ultrasound. *Nat Commun.* 2018;9:2336.
62. Rezaei AR, Ranjan M, D'Haese P-F, et al. Noninvasive hippocampal blood-brain barrier opening in Alzheimer's disease with focused ultrasound. *Proc Natl Acad Sci USA.* 2020;117:9180–9182.
63. Jönhagen ME, Nordberg A, Amberla K, et al. Intracerebroventricular infusion of nerve growth factor in three patients with Alzheimer's disease. *Dement Geriatr Cogn Disord.* 1998;9:246–257.
64. Josephy-Hernandez S, Pirvulescu I, Maira M, et al. Pharmacological interrogation of TrkA-mediated mechanisms in hippocampal-dependent memory consolidation. *PLoS One.* 2019;14:e0218036.
65. Markowska AL, Koliatsos VE, Breckler SJ, Price DL, Olton DS. Human nerve growth factor improves spatial memory in aged but not in young rats. *J Neurosci.* 1994;14:4815–4824.
66. Frick KM, Price DL, Koliatsos VE, Markowska AL. The effects of nerve growth factor on spatial recent memory in aged rats persist after discontinuation of treatment. *J Neurosci.* 1997;17:2543–2550.
67. Cooper JD, Salehi A, Delcroix JD, et al. Failed retrograde transport of NGF in a mouse model of Down's syndrome: reversal of cholinergic neurodegenerative phenotypes following NGF infusion. *Proc Natl Acad Sci USA.* 2001;98:10439–10444.
68. Schirrmacher R, Bailey JJ, Mossine AV, et al. Radioligands for tropomyosin receptor kinase (trk) positron emission tomography imaging. *Pharmaceuticals.* 2019;12:7.
69. Richter N, Beckers N, Onur OA, et al. Effect of cholinergic treatment depends on cholinergic integrity in early Alzheimer's disease. *Brain.* 2018;141:903–915.